Proceeding of the 2013
RSI/ISM International Conference on Robotics and Mechatronics
February 13-15, 2013, Tehran, Iran

Dynamics Modeling and Control of an Armed Ballbot with Stabilizer

Pouya Asgari[1]
Department Of Mechanical Engineering
K. N. Toosi Univ. Of Technology
Tehran, Iran
Po.asgari@gmail.com

S. Ali A. Moosavian[2]
Department Of Mechanical Engineering
K. N. Toosi Univ. Of Technology
Tehran, Iran
Moosavian@kntu.ac.ir

***Abstract*—The combination of mobile platform and a manipulator which is known as a mobile manipulator can be used in lots of applications. Motion control with respect to stability of dynamically stable mobile manipulators is one the interesting challenges in robotics. Mobile robots with small base are capable of moving in limited space. A Ballbot is an under-actuated system with nonholonomic dynamic constraints. It is as tall as human height until could interact by people whereas a Ballbot has not been equipped with a manipulator for grasping objects. In this paper, it has been equipped with a PUMA type manipulator which gives to the proposed robot the capability of object manipulation. Because of passive joints, Ballbot cannot maintain stability and following desired end-effector trajectory. So, a 2 DOF stabilizing pendulum is used to help the stability of a system and make the manipulator practical. As a result, dynamics equations of the assumed mobile robot are presented. Furthermore, a model-based controller is described to move the end-effector along the desired path/trajectory and maintains the system balance. Obtained results show the capabilities of the proposed control algorithm in satisfying the desired objectives.**

***Index Terms*—Ballbot, Mobile Manipulator, Stability, Motion Control**

I. INTRODUCTION

The majority of robotic research has in the last decades focused on either mobile platforms or manipulators, and there have been many impressive results within both areas. Today one of the new challenges is to combine the two areas, into systems, which are both highly mobile and have the ability to manipulate the environment. Especially within service robotics there will be an increased need for such systems [1]. A Ballbot is an under-actuated system with nonholonomic dynamic constraints. A significant, but a frequently overlooked problem is that statically-stable wheeled mobile robots can easily become dynamically unstable. If the centre of gravity is too high, or the robot accelerates are too rapidly, or is on a sloping surface, the machine can tip over [2]. To perform an object manipulation task, a manipulator should be appended to the Ballbot. This manipulator can help the Ballbot to handle an object although Existence of passive joints in body of the Ballbot makes control of the system harder.

Overall design, mechanism based on an inverse mouse-ball drive, control system, and initial results including dynamic balancing, station keeping, and point-to-point motion were described, [3]. Nagarajan and et al. presented an integrated planning and control procedure, wherein standard graph-search algorithms are used to plan for the sequence of control policies that will help the system achieve a navigation goal, [4]. Also, they proposed an offline trajectory for body (passive joints) until ball (actuated joints) could reach to its desired configuration with regard to the dynamic constraint. A fuzzy controller for the Ballbot and sliding mode control is proposed in [5] and [6].

Application of mobile manipulators had long history. In [7], the manipulator motion was discussed for stabilizing the mobile manipulator based on ZMP criterion while the mobile base is moving along a desired motion. Also, in [8] compensation motion of a redundant manipulator is derived when the mobile manipulator executes a task in which the motions of the vehicle and the manipulator's endpoint, respectively, are given. A simple controller for robot motion and an optimization method for choosing its parameters were presented in [9].

In this paper, we equipped the Ballbot with a manipulator that is the first three PUMA links. It gives the Ballbot the ability of grasping an object. Due to presence of passive joints on body of the Ballbot, 3 degrees of freedom (DOF) manipulator cannot execute the given motions of the end-effector and move the mobile manipulator stable simultaneously. So, stabilizing pendulum is used to help the stability of the system and makes the manipulator practical. At first, we obtain the complete dynamics model of Ballbot with a manipulator and a stabilizer by Lagrange method and verify it. Next, stable motion control of the system is performed to move the end-effector on desired planned path while the whole system is stable by controlling the body joints on zero position. At last, the simulation is accomplished to move the end-effector along the desired path. Obtained results of the implementation of this controller on the robot will be discussed.

1- MSc Student
2- Professor

978-1-4673-5811-8/13/$31.00 ©2013 IEEE

II. Dynamics Equations of Motion

In this section, first, the system structure and the physical configuration are described. Then, the dynamics modelling of the robot is presented by using Lagrangian and Kane mechanics. Details of modelling of the system without a stabilizer were presented in [10]. So, in this paper, we introduce the whole system with stabilizer briefly. Then, dynamic equations of motion of stabilizer are presented completely.

To describe the dynamics of the robot, a reference coordinate XYZ is selected. The robot have 9 DOF, consist of a ball with 2 DOF, 2 DOF for cylinder (roll and pitch of base, [11]), a manipulator with 3 DOF and a stabilizing pendulum with 2 DOF. The reference coordinate is selected as shown in Fig. 1. Also, θ_1 and θ_2 are considered as ball rotations about Y and X directions, respectively [10]. For body rotations, θ_3 and θ_4 are considered as roll and pitch angles of base as shown in Fig. 1.

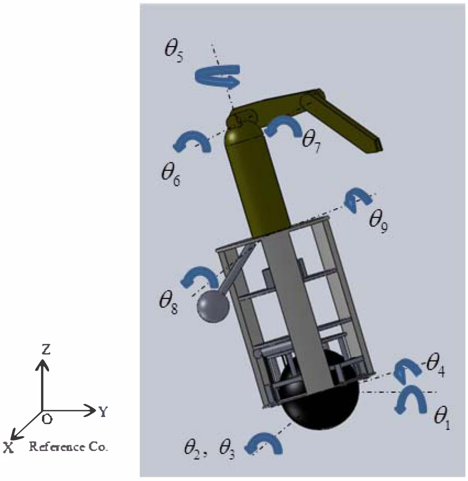

Fig 1 – Definition of the reference and generalized coordinates

2 rotations of stabilizing pendulum (θ_8, θ_9) are done about x and y directions in body coordinate (body coordinated is a coordinated which attaches to cylinder and rotates with θ_3 and θ_4). The Denavit-Hartenberg notation is used to select frames for manipulator rotations, [12]. Thus, the transformation matrix of pendulum rotation is:

$$ {}^{0}_{9}T = {}^{0}_{4}T \begin{bmatrix} c_9 & 0 & s_9 & 0 \\ s_9 s_8 & c_8 & -s_8 c_9 & 0 \\ -s_9 c_8 & s_8 & c_9 c_8 & l_B \\ 0 & 0 & 0 & 1 \end{bmatrix} \tag{1} $$

As a result, the angular velocity of coordinate 9 (for stabilizing pendulum) relative to coordinate 4 and expressed in reference coordinate is:

$$ \boldsymbol{\omega}_9 = {}^{0}_{4}R\left(\dot{\theta}_8 \quad \dot{\theta}_9 \cos\theta_8 \quad \dot{\theta}_9 \sin\theta_8\right)^T \tag{2} $$

Where ${}^{0}_{4}R$ is first three rows and columns of ${}^{0}_{4}T$ [10]. The velocity of mass j refers to reference coordinate is computed as follows:

$$ \mathbf{V}_j = \mathbf{V}_b + \sum_{i=4}^{j} \boldsymbol{\omega}_i \times {}^{0}\mathbf{P}_j^{i} \qquad j = 4,5,6,7 \tag{3} $$

Where $\mathbf{V}_b$ is the velocity of ball, ${}^{0}\mathbf{P}_j^{i}$ is the position vector of mass j refers to coordinate i and expressed in reference coordinate and $j = 4,5,6,7$ is for COG of body, COG of first, second and third manipulator link respectively. Velocity of the ball is obtained as follows:

$$ \mathbf{v}_b = r\dot{\theta}_1 \mathbf{i} - r\dot{\theta}_2 \mathbf{j} \tag{4} $$

To obtain ${}^{0}\mathbf{P}_j^{i}$, we act as follows:

Positions of COG of body and manipulator links in their own coordinates are as follows:

$$ \begin{aligned} \mathbf{P}_{body} &= [0 \quad 0 \quad l_{cB}]^T \\ \mathbf{P}_{first\ manipulator\ link} &= [0 \quad 0 \quad l_{c1} - (l_B + l_1)]^T \\ \mathbf{P}_{second\ manipulator\ link} &= [l_{c2} \quad 0 \quad -b_3]^T \\ \mathbf{P}_{third\ manipulator\ link} &= [l_{c3} \quad 0 \quad 0]^T \end{aligned} \tag{5} $$

Where l_{cj} is position of COG of body and manipulator links. SO, ${}^{0}\mathbf{P}_j^{i}$ is obtained from equation below:

$$ {}^{0}\mathbf{P}_j^{i} = {}^{0}_{j}T\left[\mathbf{P}_j \quad 1\right]^T - {}^{0}_{i}T(1:4,4) \qquad j = 4,5,6,7 \tag{6} $$

Where $\mathbf{P}_j$ is achieved from Eq. 5 that $j = 4,5,6,7$ is for body and first, second and third manipulator links, respectively. The velocity of pendulum is computed by

$$ \begin{aligned} \mathbf{V}_P &= \mathbf{V}_b + \boldsymbol{\omega}_4 \times {}^{0}\mathbf{P}_9^{4} + \boldsymbol{\omega}_9 \times {}^{0}\mathbf{P}_9^{9} \\ {}^{0}\mathbf{P}_9^{4} &= {}^{0}_{9}T\left[P_9^9 \quad 1\right]^T - {}^{0}_{4}T(1:4,4) \\ {}^{0}\mathbf{P}_9^{9} &= {}^{0}_{9}T\left[P_9^9 \quad 1\right]^T - {}^{0}_{9}T(1:4,4) \\ \mathbf{P}_9^9 &= \left[0 \quad 0 \quad -l_5\right]^T \end{aligned} \tag{7} $$

Where $\mathbf{P}_9^9$ is the position of COG of stabilizing pendulum in its own coordinate (coordinate 9).

The ball is actuated by a pair of smooth stainless steel rollers placed orthogonally at the sphere's equator. The manipulator's link and stabilizing pendulum are rotated by motors that apply torque to each links. So, Non-potential forces for system are:

$$ \left[\frac{r_b}{r_s} s_3 s_4 \tau_1 + \frac{r_b}{r_s} c_3 \tau_2 \quad \frac{r_b}{r_s} c_4 \tau_1 \quad -\frac{r_b}{r_s} c_4 \tau_1 \quad -\frac{r_b}{r_s} \tau_2 \quad \tau_5 \quad \tau_6 \quad \tau_7 \quad \tau_8 \quad \tau_9\right]^T \tag{8} $$

where τ_1, τ_2 are torques of rollers, τ_5, τ_6, τ_7 are torques of manipulator [10] and τ_8, τ_9 are torques of stabilizing pendulum. Pendulum is considered as intensive mass so the inertia of momentum of pendulum is zero.

A. Lagrange's Equations

The forced Lagrange equations of system without stabilizer were presented in [10]. The potential and the kinetic energy of the stabilizing pendulum should be computed and added to Lagrange function. The kinetic energy of the stabilizer is obtained from Eq. 9.

$$T = 0.5(m_P \mathbf{V}_P{}^T \mathbf{V}_P) \tag{9}$$

Where m_P refer to the mass of pendulum and $\mathbf{V}_P$ refer to velocity of the center of mass of stabilizing pendulum which is achieved from Eq. 7, we note that because a pendulum is considered as intensive mass, so the inertia of momentum of pendulum is zero and angular kinetic energy of pendulum is zero. Also, the potential energy of the pendulum is computed as follows:

$$\mathrm{V} = m_P \mathbf{g}^T \bar{R}_P \tag{10}$$

Where $\mathbf{g} = [0 \quad 0 \quad 9.81]^T$ and $\bar{R}_P$ is the center gravity's position of pendulum refer to coordinate 0.

B. Kane's Equations

Details of Kane's equations without pendulum were presented in [10]. In presence of stabilizing pendulum, linear and angular velocities and accelerations are obtained from Eq. 11.

$$\mathbf{v}_i = \begin{bmatrix} \mathbf{v}_{Gi} \\ \boldsymbol{\omega}_i \end{bmatrix} = J_i \dot{q}$$
$$\mathbf{a}_i = \begin{bmatrix} \mathbf{a}_{Gi} \\ \boldsymbol{\alpha}_i \end{bmatrix} = \dot{J}_i \dot{q} + J_i \ddot{q} \tag{11}$$
$$q = [\theta_1 \quad \theta_2 \quad \theta_3 \quad \theta_4 \quad \theta_5 \quad \theta_6 \quad \theta_7 \quad \theta_8 \quad \theta_9]^T$$

C. Model Verification

In this section, comparison of two analytical methods (Lagrange and Kane) is used to reveal the validity of the model. Arbitrary trajectory is applied to each joint according to Eq. 12. Then, actuator torques of all active joints is achieved by Lagrange and Kane method. The difference between obtained results shows errors of dynamic model. Torques of each joint which is obtained from Lagrange method is shown in Fig. 2. Errors are shown in Fig. 3. It would be obvious that errors are in order of 10^{-15} that reveals two models are completely the same.

$$\theta_i = 6\sin(\frac{t}{2\pi}) \qquad i = 1,2,5,6,7$$
$$\theta_i = 0.1\sin(\frac{t}{2\pi}) \qquad i = 3,4 \quad , \theta_i = 0.5\sin(\frac{t}{2\pi}) \qquad i = 8,9 \tag{12}$$

Mass of body, mass of pendulum and length of pendulum are considered 5 kg, 3 kg and 0.5 m, respectively. All other parameters were presented in [10].

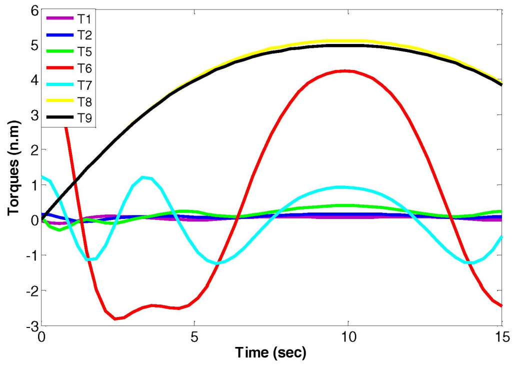

Fig. 2: Calculated actuator torques of each joint by Lagrange method

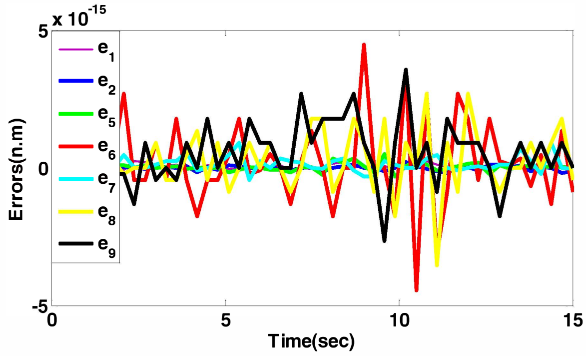

Fig. 3: Comparison results of Lagrange and Kane method

III. STABILIZING PENDULUM

The Ballbot is an underactuated system, systems with fewer control inputs than the number of generalized coordinates. Although adding a manipulator to the Ballbot gives the Ballbot the ability of grasping, it is not possible to control the end-effector and stability of the system, simultaneously. Ballbot with manipulator have 7 DOF with 5 actuators. When the manipulator moves in space, centre of gravity of whole system changes and Existence of passive joints in body of Ballbot causes that the system being unstable by changing the position of centre of gravity. So, the system should be equipped to a stabilizer to help the stability of the system and give permission to manipulator to move freely. A pendulum with 2 DOF brings this possibility to the system.

IV. PLANNING

Quintic polynomial path is defined as end-effector trajectory. The initial and final position of end effector is $\mathbf{P_0} = [0.71 \quad 0.1 \quad 0.86]^T$ and $\mathbf{P}_g = [3 \quad 3 \quad 1.8]^T$. This path is be mapped from workspace to joint space by inverse kinematic. Two different trajectories are defined in joint space.

A. Ball joints and second manipulator link

First, planning has been done how only ball joints (θ_1, θ_2) and second manipulator link (θ_6) participate in end-effector placement and other joints remain on their initial position. Schematic of first and last configuration of the system is shown in Fig. 4. Joints, which participate in motion, are colored with green.

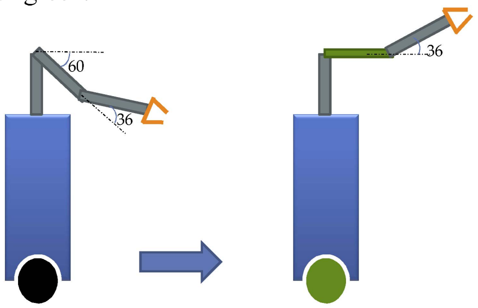

Fig. 4: Schematic of first and last position of the system in first movement

Quintic polynomial path in work space will be

$$\begin{cases} x = 0.00013t^5 - 0.0034t^4 + 0.023t^3 + 0.71 \\ y = 0.00017t^5 - 0.0043t^3 + 0.029t^3 + 0.1 & 0 \le t \le 10 \\ z = 0.00056t^5 - 0.0014t^4 + 0.009t^3 + 0.8636 \end{cases} \tag{13}$$

By mapping this path in joint space, joints trajectory are shown in Fig. 5.

B. First ball joints and then manipulator links

In this section Quintic polynomial path is mapped to joint space how first ball joints move to near the goal position, $\mathbf{P}_v = [2.5 \quad 2.5 \quad 0]^T$, then ball stops and 3 manipulator links reach end-effector to its final position. Ball moves to $\mathbf{P}_v = [2.5 \quad 2.5 \quad 0]^T$ in first 7 seconds as Eq. 14

$$\begin{cases} \theta_1 = 0.0044t^5 - 0.078t^4 + 0.364t^3 \\ \theta_2 = -0.0044t^5 + 0.078t^4 - 0.364t^3 \end{cases} \quad 0 \le t \le 7 \tag{14}$$

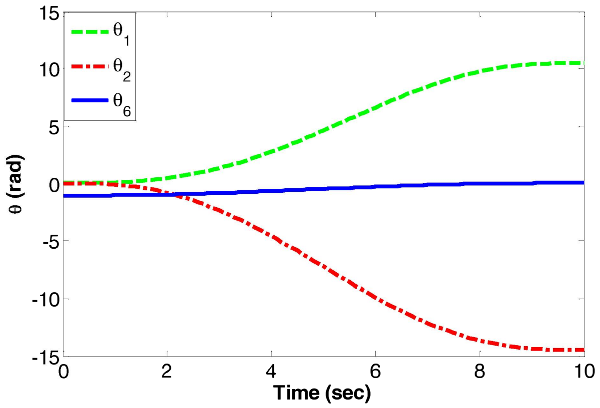

Fig. 5: Ball and second manipulator joint trajectory

In last 3 seconds, end-effector path will be:

$$\begin{cases} X = -0.0051(t-7)^5 + 0.038(t-7)^4 - 0.076(t-7)^3 + 0.7068 \\ Y = 0.0099(t-7)^5 - 0.0741(t-7)^4 + 0.148(t-7)^3 + 0.1 & 7 \le t \le 10 \\ Z = 0.023(t-7)^5 - 0.173(t-7)^4 + 0.347(t-7)^3 + 0.8636 \end{cases} \tag{15}$$

Schematic configuration of the system at the beginnig and end of the movement is displayed in Figure below. Manipulator joints that move in last 3 seconds are colored with green.

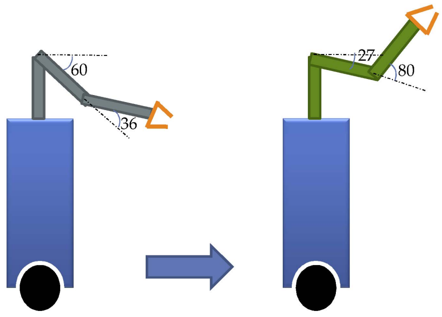

Fig. 6: Schematic of first and last position of the system in second movement

By mapping this path in joint space, trajectory of manipulator links are based on Fig. 7

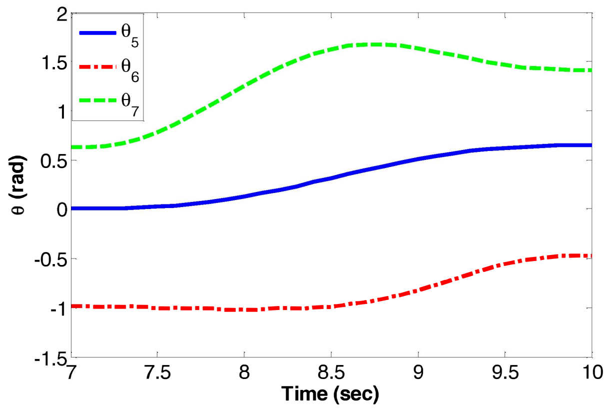

Fig. 7: Manipulator joints trajectory in last 3 seconds

V. Controller Design

Underactuated systems contain both active and passive joints in a serial kinematics chain. It has long been known that fully actuated robots are feedback linearizable by nonlinear feedback. Spong in [13] using partial feedback to linearized the portion of the dynamics corresponding to the passive degrees of freedom. In [14] authors controlled passive joints of a manipulator by motion of active joints that was used coupling characteristics. Furthermore, Arai, Tanie and Tachi presented a method to control an underactuated manipulator in operation space by using coupling characteristics of manipulator dynamics [15].

In this section, manipulator is controlled on desired path. If body joints (θ_3, θ_4) are controlled at zeros as desired position, the whole system will become stable. Thus, stabilizer is used to control the body joints at zeros. By this action, manipulator can move on desired position while the system is stable. A model-based controller is used to control the body joints and end-effector position. This controller uses dynamic model of the system to create the control command and force the system to move on chosen trajectory.

As θ_3, θ_4 are controlled at 0 during the control process, $\cos\theta_i \cong 1,\ \sin\theta_i \cong 0\ \ i=3,4$ and right side of Eq. 8 will be:

$$\tau' = [\tau'_2 \quad \tau'_1 \quad -\tau'_1 \quad -\tau'_2 \quad \tau_5 \quad \tau_6 \quad \tau_7 \quad \tau_8 \quad \tau_9]^T \tag{16}$$

$$\tau'_1 = \frac{r_b}{r_s}\tau_1, \qquad \tau'_2 = \frac{r_b}{r_s}\tau_2$$

So, by adding rows first and forth, and rows second and third, dynamic equations are written in form of Eq. 17

$$M'\ddot{q} + C' = \tau'$$
$$M' = \begin{bmatrix} M_1 & M_2 \\ M_3 & M_4 \end{bmatrix} \tag{17}$$

$$C' = \begin{bmatrix} C_1 \\ C_2 \end{bmatrix}$$

$$\tau' = [\tau'_2 \quad \tau'_1 \quad \tau_5 \quad \tau_6 \quad \tau_7 \quad \tau_8 \quad \tau_9 \quad 0 \quad 0]^T$$

Where $M_1 \in \mathbb{R}^{7\times7}, M_2 \in \mathbb{R}^{7\times2}, M_3 \in \mathbb{R}^{2\times7}, M_4 \in \mathbb{R}^{2\times2}, C_1 \in \mathbb{R}^{7\times1}, C_2 \in \mathbb{R}^{2\times1}$ Eq. 17 can be written as Eq. 18, Eq. 19

$$M_1\ddot{q}_o + M_2\ddot{q}_p + C_1 = [\tau'_2 \quad \tau'_1 \quad \tau_5 \quad \tau_6 \quad \tau_7 \quad \tau_8 \quad \tau_9]^T \tag{18}$$

$$M_3\ddot{q}_o + M_4\ddot{q}_p + C_2 = 0 \tag{19}$$

Where $q_o = [\theta_1 \quad \theta_2 \quad \theta_3 \quad \theta_4 \quad \theta_5 \quad \theta_6 \quad \theta_7]^T, q_p = [\theta_8 \quad \theta_9]^T$. By replacing $\ddot{q}_p$ from Eq. 19 to Eq. 18:

$$\begin{aligned} &\bar{M}\ddot{q}_o + \bar{C} = \bar{\tau} \\ &\bar{M} = M_1 - M_2 M_4^{-1} M_3 \\ &\bar{C} = -M_2 M_4^{-1} C_2 + C_1 \\ &\bar{\tau} = [\tau'_2 \quad \tau'_1 \quad \tau_5 \quad \tau_6 \quad \tau_7 \quad \tau_8 \quad \tau_9]^T \end{aligned} \tag{20}$$

If torque of active joints exert to the system based on Eq. 21, q_0 will track its desired position.

$$\begin{aligned} &\bar{\tau} = \tilde{M}u_1 + \tilde{C} \\ &u_1 = \ddot{q}_{do} + k_v(\dot{q}_{do} - \dot{q}_o) + k_p(q_{do} - q_o) \end{aligned} \tag{21}$$

VI. Simulation Results And Discussion

The system is controlled on desired path which was designed in IVA and IVB. For the first section (IVA), Error of each joint is shown in Fig. 8. It would be obvious that all joints tracked their desired trajectories perfectly. It shows that control input can control the system in its desired path flawlessly. Position of stabilizing pendulum is displayed in Fig. 9. A pendulum has limited space in body of the system and always should be checked to not hit with the inner surface of the body. According to the stabilizer movement, stabilizer moves maximum about 0.24 m related to body of the Ballbot. This movement is lower than 0.3 m radius of body. So, there is no problem for stabilizer movement and it can move in the body of the Ballbot freely. A schematic motion of the system is shown in Fig. 10.

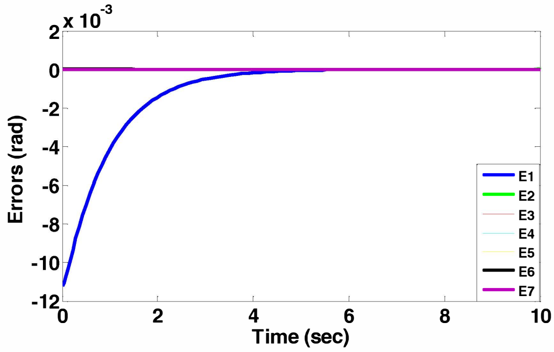

Fig. 8: Joints error when ball and second manipulator joint move

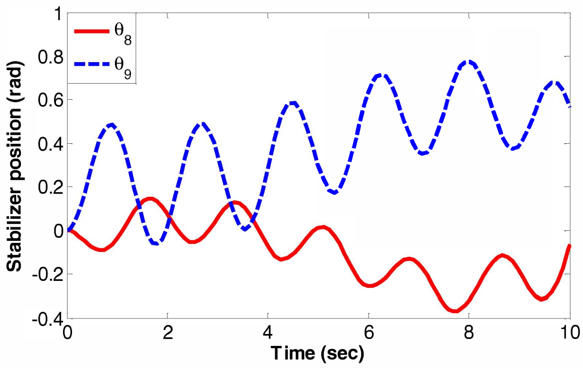

Fig. 9: stabilizer position when ball and second manipulator joint move

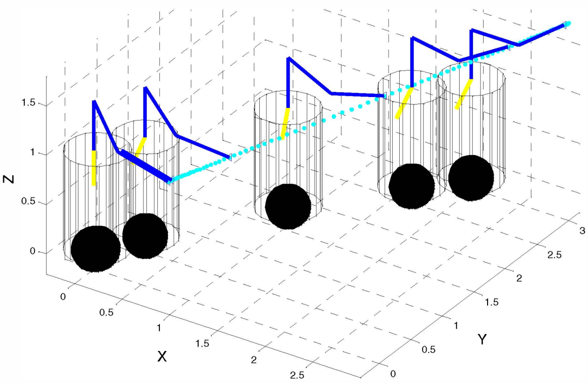

Fig. 10: Schematic motion when ball and second manipulator joint move

For second section (IVB), all joints follow their trajectories and stabilizer position shows that the pendulum stabilizes the whole system in its limited space and without hit to the inner surface of the body of the Ballbot (Calculation shows that pendulum moves maximum 0.23 m related to body of the Ballbot) (Fig. 12). Error of all joints reached at zero, perfectly and reveals accuracy of the control algorithm (Fig. 11). A spring that would be obvious in 7th second is related to change in joints trajectory from ball motion to manipulator motion. Finally, animated view of the system is shown in Fig. 13.

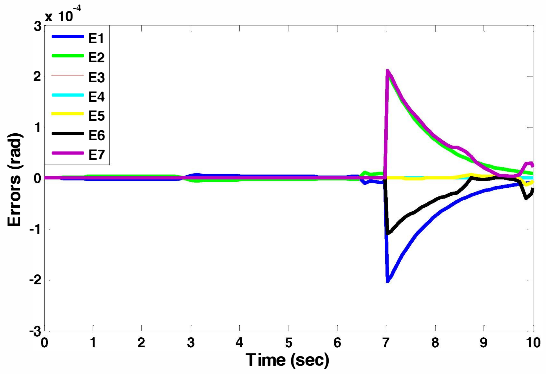

Fig. 11: Joints error when first ball then manipulator links moves

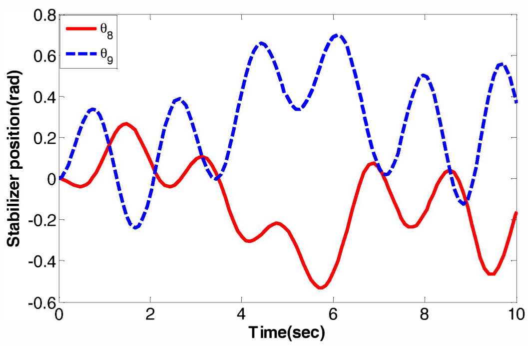

Fig. 12: Stabilizer position when first ball then manipulator links moves

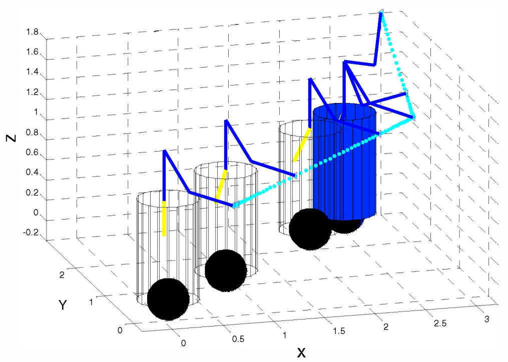

Fig. 13: schematic motion when first ball then manipulator links moves

VII. Conclusions

This paper was presented dynamics model and stable motion control of a Ballbot which is equipped with a manipulator and stabilizer. Manipulator could help the Ballbot to handle an object. A stabilizer was added to maintain the stability of the whole system because when the end-effector tracked the desired position, it disturbs system balance and existence of passive joints in body of the Ballbot. So, it causes the system couldn't be stable. To apply a stable motion control, a controller was used to control the whole system. This action was done by controlling the end-effector position and position of body joints at zero. Finally, simulation results were shown that the proposed control scheme could control the system well.

References

[1] Ellekilde, L., Christensen, H.," Control of Mobile Manipulator using the Dynamical Systems Approach," IEEE International Conference on Robotics and Automation, Kobe, Japan, pp. 1370-1376 (2009)

[2] T. Lauwers, G. A. Kantor, and R. Hollis, "A dynamically stable single-wheeled mobile robot with inverse mouse-ball drive," in Proceedings of the IEEE International Conference on Robotics and Automation, Orlando, FL, USA, 2006, pp. 2884-2889.

[3] T. Lauwers, G. Kantor, and R. Hollis, "One is enough!," Robotics Research, pp. 327-336, 2007.

[4] U. Nagarajan, G. Kantor, and R. Hollis, "Hybrid control for navigation of shape-accelerated underactuated balancing systems," in 49th IEEE Conference on Decision and Control, Atlanta, GA, 2010, pp. 3566-3571.

[5] Y. F. Peng, C. H. Chiu, W. R. Tsai, and M. H. Chou, "Design of an Omni-directional Spherical Robot: Using Fuzzy Control," 2009.

[6] C. W. Liao, C. C. Tsai, Y. Y. Li, and C. K. Chan, "Dynamic modelling and sliding-mode control of a Ball robot with inverse mouse-ball drive," in SICE Annual Conference, Tokyo, Japan, 2008, pp. 2951-2955.

[7] Q. Huang, and S. Sugano, "Manipulator Motion Planning for Stabilizing a Mobile-Manipulator," IEEE, pp. 467-472, 1995

[8] Q. Huang, K. Tanie, and S. Sugano, "Stability compensation of a mobile manipulator by manipulator motion: Feasibility and planning," Advanced robotics, vol. 13, pp. 6-8, 1999.

[9] M. Stilman, J. Wang, K. Teeyapan, and R. Marceau, "Optimized control strategies for wheeled humanoids and mobile manipulators," in Proceedings of the IEEE-RAS International Conference on Humanoid Robots, Paris, 2009, pp. 568-573.

[10] P. Asgari, P. Zarafshan, and S. A. A. Moosavian, "Dynamics Modeling and Stable Motion Control of a Ballbot Equipped with a Manipulator," presented at the RSI/ISM International Conference on Robotics and Mechatronics (ICROM), Tehran, Iran, 2013.

[11] L. Meirovitch, Methods of analytical dynamics: Dover Publications, 2010.

[12] J. J. Craig, "Introduction to Robotics. Mechanics and Control. Series in Electrical and Computer Engineering: Control Engineering," ed: Addison-Wesley, Reading, MA, USA, 1989.

[13] M. W. Spong, "Partial feedback linearization of underactuated mechanical systems," 1994, pp. 314-321.

[14] H. Arai and S. Tachi, "Position control of manipulator with passive joints using dynamic coupling," Robotics and Automation, IEEE Transactions on, vol. 7, pp. 528-534, 1991.

[15] H. Arai, K. Tanie, and S. Tachi, "Dynamic control of a manipulator with passive joints in operational space," Robotics and Automation, IEEE Transactions on, vol. 9, pp. 85-93, 1993.